

1 Mechanisms of burst release from pH-responsive polymeric 2 microparticles.

3 Khalida Rizi ^a, Rebecca J. Green ^a, Olga Khutoryanskaya^a, Michael Donaldson^b, Adrian C. Williams ^{a,*}

4 ^a Reading School of Pharmacy, University of Reading, Whiteknights, P.O. Box 226, Reading RG6 6AP,
5 UK

6 ^b Stiefel Laboratories, Eurasia Headquarters, Concorde Road, Maidenhead, SL6 4BY, UK

7 *Corresponding author. Tel: +44 0 118 378 6196; Fax: +44 0 118 378 6562.E-mail:
8 a.c.williams@reading.ac.uk

9 Abstract

10 Microencapsulation of drugs into preformed polymers is commonly achieved through solvent
11 evaporation techniques or spray drying. We compared these encapsulation methods in terms of
12 controlled drug release properties of the prepared microparticles and investigated the underlying
13 mechanisms responsible for the “burst release” effect. Using two different pH-responsive polymers
14 with a dissolution threshold of pH 6 (Eudragit L100 and AQQAT AS-MG), hydrocortisone, a model
15 hydrophobic drug, was incorporated into microparticles below and above its solubility within the
16 polymer matrix. Although, spray drying is an attractive approach due to rapid particle production
17 and relatively low solvent waste, the oil-in-oil microencapsulation method is superior in terms of
18 controlled drug release properties from the microparticles. Slow solvent evaporation during the oil-
19 in-oil emulsification process allows adequate time for drug and polymer redistribution in the
20 microparticles and reduces uncontrolled drug burst release. Electron microscopy showed that this
21 slower manufacturing procedure generated non-porous particles whereas thermal analysis and X-ray
22 diffractometry showed that drug loading above the solubility limit of the drug in the polymer
23 generated excess crystalline drug on the surface of the particles. Raman spectral mapping illustrated
24 that drug was homogeneously distributed as a solid solution in the particles when loaded below
25 saturation in the polymer with consequently minimal burst release.

26

27 **Key words:** Oil in water, oil in oil, microencapsulation, spray drying, Eudragit L100, burst release,
28 hydrocortisone.

29 **1 Introduction**

30 Polymeric microparticles are increasingly used for controlled drug delivery. Preparation of these
31 microparticles from pre-formed polymers is based on modifications of three basic methods; solvent
32 extraction/evaporation, phase separation (coacervation) and spray-drying ^[1]. The emulsification
33 solvent evaporation approach is a simple and widely applied technique, extensively studied for the
34 preparation of polylactic acid (PLA) and poly(lactic-co-glycolic) acid (PLGA) microparticles ^[2,3].
35 However, this technique uses relatively large amounts of solvents and results in a suspension of
36 microparticles in the external phase ^[4-6]. To acquire a dry powder further processing, such as
37 filtration or lyophilisation, is needed. Another frequent problem encountered using conventional
38 emulsification methods is drug crystallisation in the external continuous phase ^[6]. This problem was
39 overcome in the case of progesterone-loaded polylactide microspheres using a spray drying method,
40 hot air being the external phase ^[7].

41 With regards to controlled-release properties, one of the difficulties often reported for polymeric
42 microparticles is an initial high drug release from the polymer matrix, known as a “burst release
43 effect” ^[5, 8-13]. In an attempt to explain this phenomenon, a number of theories have been suggested.
44 Wang et al. (2002) related drug release to the density of the produced microparticles suggesting that
45 denser particles result in lower release rates ^[11]. Other authors attributed the burst release to high
46 residual solvent, reduced glass transition temperature, surface drug enrichment or insufficient
47 encapsulation ^[13-16]. In fact, it is well established that the distribution of drugs in delivery systems
48 influences the release characteristics ^[15]. However, this is often hard to quantify *in-situ* and detailed
49 investigations into the mechanisms responsible for the burst release effect in various
50 microencapsulation methods have not been reported.

51 This work evaluates microencapsulation methods in terms of optimal controlled-release
52 characteristics and uses various analytical techniques to investigate the possible underlying
53 mechanisms causing burst- or controlled-release properties. Two different pH-responsive polymers
54 with a dissolution threshold of pH 6 (Eudragit L100 and AQOAT AS-MG) were used to encapsulate
55 hydrocortisone, a model hydrophobic drug, into microparticles below and above its solubility within
56 the polymer matrix. Varying the drug loading above and below the solubility within the polymer
57 tests whether drug encapsulation using spray drying is only marginally dependent on the drug’s
58 affinities to the solvent and polymer used ^[7]. Raman microscopy was then used to investigate the
59 spatial distribution of the drug within the produced microparticles which was related to
60 experimental release profiles. Unlike previous studies which develop pH-responsive microparticles
61 intended for gastro-intestinal drug delivery, the goal of this work was to develop controlled delivery

62 systems which respond to more subtle pH changes, such as those observed in healthy (pH 5.0-5.5)
63 versus atopic dermatitis skin (6.0-7.0) ^[17, 18].

64 **2 Materials and methods**

65 **2.1 Materials**

66 Hydrocortisone was purchased from Sigma-Aldrich (UK). Eudragit L100 was kindly provided by Röhm
67 (Germany). Hypromellose acetate succinate (HPMCAS) (AQOAT[®] AS-MG) was obtained from Shin-
68 Etsu (Tokyo, Japan). Ethanol, dichloromethane (DCM), hexane (laboratory grades) and sorbitan
69 sesquioleate were obtained from Sigma-Aldrich (UK). Sodium dodecyl sulphate and Liquid Paraffin
70 BP were purchased from Fisher Scientific (UK). Sodium phosphate dibasic heptahydrate and sodium
71 phosphate monobasic dehydrate (Sigma-Aldrich, UK) were used in the preparation of the dissolution
72 media.

73 **2.2 Production of pH-responsive microparticles**

74 **2.2.1 Spray drying**

75 Microparticles were produced using a Mini Spray Dryer, Model 290 (Buchi UK Ltd) under constant
76 operating conditions for different microparticles. The 50:50 w/w ethanol/water polymeric solutions,
77 with or without the drug, were fed into the machine by a peristaltic pump at 1.5 ml/min (feed rate
78 5%) and sprayed through a 0.7mm two-fluid nozzle into the drying chamber. The flow of compressed
79 nitrogen used to atomise the feed solution was 350 L/min. Inlet temperature was set at 70° C with a
80 corresponding outlet temperature of ~35° C. A flow of heated nitrogen, at 28 m³/hr (aspirator rate
81 75%), induced rapid evaporation of solvent from the droplets and led to the formation of solid
82 microparticles which were collected in a high performance cyclone. In all cases the concentration of
83 the polymer in the feed solution was maintained at 2% w/w (to circumvent changes that can arise
84 from differences in feed solution viscosity) while varying hydrocortisone loading at 2.5, 10 and 25%
85 w/w with respect to polymer.

86 **2.2.2 Solvent-evaporation method**

87 Two variations of the solvent evaporation method were investigated in this study using different
88 external phases, either water (oil in water emulsification) or liquid paraffin (oil in oil emulsification).
89 For the oil in water microencapsulation method, 10% w/v polymeric organic solutions were
90 prepared by dissolving the polymer in a mixed solvent of DCM/ ethanol (7:3 v/v). This solution (10
91 ml) was added to 100 ml of 0.25% w/v hydroxypropyl methylcellulose (HPMC) aqueous phase.
92 Similarly, with the oil in oil method, 15 ml of 10% w/v polymer ethanolic solution (oil₁) was

93 emulsified into 100 ml liquid paraffin (oil₂) containing 1% w/w of sorbitan sesquioleate as an
94 emulsifying agent^[19].

95 For both techniques, the emulsion was obtained by stirring (4 cm four-blade propeller) at 1200 rpm
96 (IKA[®] Laboratechnik). Solvent removal was achieved by continuous stirring of the emulsion droplets
97 at 1200 rpm overnight at room temperature to allow solvent evaporation. The solidified
98 microparticles were then recovered by vacuum filtration (through Whatman filter paper, 0.45 μm
99 pore size), washed with 200 ml of water in the case of the oil-in-water emulsification or with three
100 portions of 25ml *n*-hexane after the oil-in-oil microencapsulation process. This was followed by
101 vacuum drying for 6 hrs at room temperature. 2.5%, 10% and 25% w/w hydrocortisone-loaded
102 microparticles were obtained by incorporating the appropriate drug amount to the initial polymeric
103 solutions.

104 **2.3 Yield and encapsulation efficiency**

105 Microparticle yields were calculated by:

$$106 \quad Yield = \frac{W_{recovered}}{W_{total}} \times 100 \quad \text{Equation 1}$$

107
108 Where, W_{total} is the total solids weight used in the initial polymeric solution and $W_{recovered}$ is the
109 weight of recovered microparticles. To calculate drug encapsulation efficiency, amounts of dry
110 powder samples equivalent to 20 μg/ml theoretical hydrocortisone loading were dissolved in
111 ethanol for Eudragit L100 microparticles and in pH7 phosphate buffer for AQOAT AS-MG (as this
112 polymer is insoluble in ethanol). The amount of hydrocortisone encapsulated was determined by UV
113 spectrophotometry (Jasco V-530 UV-VIS spectrophotometer) at 242 nm (ethanol) or 248 nm (pH 7
114 phosphate buffer) against calibration curves. The encapsulation efficiency (EE) was calculated as:

$$115 \quad EE = \frac{M_{actual}}{M_{theoretical}} \times 100 \quad \text{Equation 2}$$

116 Where, M_{actual} is the actual amount of the drug encapsulated and $M_{theoretical}$ is the theoretical
117 amount encapsulated, calculated from the amount of drug added during the manufacturing process.
118 All analyses were performed in triplicate.

119 **2.4 Scanning electron microscopy**

120 Scanning electron microscopy (SEM) was used to examine the shape and surface morphology of the
121 microparticles. Powder samples were attached to double sided adhesive carbon tabs mounted on an

122 SEM support, coated with gold (Edwards Sputter Coater S150B) and assessed with a high vacuum
123 scanning electron microscope (SEM) (Cambridge 360 stereoscan). The SEM instrument was operated
124 at an accelerating voltage of 20 KeV and a working distance of about 15 mm.

125 **2.5 Density**

126 Bulk density (bp) was measured by filling the dry powder into a 2 ml graduated syringe whose
127 bottom was sealed with Parafilm™ [20, 21]. The weight and volume occupied by the powder was
128 recorded to calculate bp. The tap density (tp) of the powders was then evaluated by tapping the
129 syringe onto a level surface at a height of about 2 cm [20], until no change in volume was observed.
130 The resultant volume was then recorded to calculate tp. Each measurement was performed in
131 triplicate.

132 **2.6 Thermo-gravimetric Analysis (TGA)**

133 Thermo-gravimetric analysis assessed the residual solvent within the prepared microparticles. These
134 investigations were performed in a Q50 TA instrument (TA Instruments Ltd, UK) equipped with TA
135 universal analysis software. Samples of about 10 mg were heated from 30 to 200°C at 20°C /minute
136 under a nitrogen purge of 50 ml/min using a platinum pan.

137 **2.7 Differential scanning calorimetry (DSC)**

138 Thermal behaviour of polymers, drug, drug free microparticles and drug-loaded microparticles was
139 analysed using differential scanning calorimetry (Q2000 TA instruments) equipped with TA universal
140 analysis software. The apparatus was calibrated with indium prior to analysis. Approximately 4 mg
141 samples were accurately weighed into standard aluminium pans, which were then crimped and
142 heated from 30 to 150°C at 10°C/minute with a 30 min isothermal hold at 150°C to remove any
143 excess moisture. The samples were then cooled to 30°C and heated to 250°C at 10°C /minute under
144 a nitrogen purge of 20ml/min. All samples were tested in triplicate.

145 **2.8 X-ray powder diffraction (XRPD) measurements**

146 X-ray powder diffraction patterns of the starting materials (hydrocortisone and Eudragit L100) and
147 microparticles were obtained using a Bruker D8 Advance diffractometer (Bruker, Germany), using Cu
148 K α radiation ($\lambda = 1.5406 \text{ \AA}$). Samples were scanned from 5 to 45° 2 θ , with a step size of 0.017° and a
149 count time of 3 seconds per step. Samples were rotated at 30 rpm during analyses. The generator
150 was set to 40 keV and 40 mA.

151 **2.9 Raman microscopy**

152 Raman spectra were recorded using a dispersive Renishaw inVia Raman microscope coupled with a
153 532 nm diode laser source and a Leica DM2500 M microscope. A 100 x working-length objective was

154 used for optical imaging and spectral acquisition. The collected radiation was directed through a
155 notch filter that removes the Rayleigh photons, then through a confocal hole and the entrance slit
156 onto a grating monochromator (2400 groove/mm) that disperses the light before it reaches the
157 charge-coupled device (CCD) detector. The spectrograph was set to provide a spectral range of 100-
158 2000 cm^{-1} .

159 Depth profiling of the oil-in-oil generated microparticles was acquired at a step of 2 μm for the 25%
160 hydrocortisone-loaded microparticles and a step of 0.8 μm for 10% and 2.5% w/w loaded-
161 microparticles. Spectrum acquisition times were typically 180s. Spectra were collected to a total
162 depth of 15.20 μm , for the 2.5% and 10% w/w hydrocortisone-loaded microparticles, and 38 μm for
163 25% hydrocortisone-containing microparticles due to their larger particle diameters. In all cases, a
164 total of 20 spectra were acquired starting from the microparticle's surface.

165 **2.10 In vitro dissolution testing**

166 pH-stepped dissolution testing of the different drug-containing microparticles was performed using
167 USP II apparatus (paddles) (Varian VK7010 dissolution system) at 50 rpm and $32\pm 1^\circ\text{C}$ (which
168 represents normal skin temperature as the microparticles are intended for topical drug delivery).
169 The reported aqueous solubility of hydrocortisone is 0.28 mg/ml^[18, 22]. Therefore, amounts of drug-
170 containing microparticles equivalent to 0.02 mg/ml hydrocortisone on complete dissolution were
171 used, ensuring sink conditions ($C < 0.1 C_s$). The powders were first tested in 500 ml of 0.1M pH 5
172 phosphate buffer for two hours, after which the pH was increased to 7 by the addition of 100 ml
173 0.29M NaOH, and testing then continued for a further two hours. Samples (1 ml) were withdrawn
174 periodically, passed through a 0.45 μm membrane filter (Millipore®) and assayed by UV
175 spectrophotometry at 248 nm, a wavelength at which no interference from the polymers was
176 observed.

177 **2.11 Statistical analysis**

178 Differences in tap density measurements and maximum drug release between Eudragit L100
179 microparticles obtained from the two methods (spray drying and solvent evaporation) and
180 containing different drug-loadings were assessed using one way analysis of variance, (Genstat;
181 version 12); in all cases $p < 0.05$ denoted significance.

182 **3 Results and discussion**

183 Unlike the solvent evaporation technique, encapsulation using spray drying is thought to be only
184 slightly dependent on the drug's compatibility with the solvent and polymer used^[7]. In this study,

185 the effect of drug:polymer compatibility on hydrocortisone release from the prepared microparticles
186 was explored by incorporating the drug at levels below and above its solubility limit within the
187 polymer matrices. The solubility of hydrocortisone in Eudragit L100 and AQQAT AS-MG was found
188 through microscopic examination of polymer films ^[23]. A high solubility of the drug in the polymer
189 matrix is indicative of high drug-polymer compatibility ^[6, 23] and results in better incorporation of the
190 drug within the prepared microparticles. Hydrocortisone was found to be more soluble (13-14%
191 w/w) in Eudragit L100 films ^[24] compared to AQQAT AS-MG (9-10% w/w; Figure 1).

192 INSERT Figure 1

193 Various other parameters including the physicochemical properties of both drug and polymer need
194 to be considered for successful encapsulation of drugs into polymeric microparticles. The model
195 drug used, hydrocortisone, has a reported water solubility of 0.28 mg/ml ^[16], and we previously
196 reported its solubility in ethanol to be 11.4±0.33 mg/ml ^[24]. These solubility's dictate the extent of
197 drug diffusion to the surface of the microparticles during the preparation process and ultimately
198 affect drug release.

199 **3.1 Preparation of pH-responsive microparticles**

200 **3.1.1 Spray drying as a microencapsulation technique**

201 We previously reported the potential use of spray drying to prepare pH-responsive Eudragit L100
202 microparticles ^[24]. The method was optimised in terms of drug release, taking into account the effect
203 of different solvent systems and various polymer concentrations. Using Eudragit L100 as a pH-
204 responsive polymer, it was found that a polymer content of 2% w/w and a solvent system of 1:1 w/w
205 ethanol/water led to the lowest drug release at pH 5, a pH at which the polymer is not soluble. Using
206 these optimised conditions, the effect of varying the drug loading (2.5% and 25% w/w) on the
207 release profile was investigated ^[24]. Here, we also report the effect of 10% w/w hydrocortisone-
208 loading (Table 1). AQQAT AS-MG microparticles were also generated using the same conditions to
209 explore the methods' transferability to other polymers (Table 1). Encapsulation efficiency was high,
210 with more than 88% of the drug incorporated in all cases. Morphological characteristics of Eudragit
211 L100 and AQQAT AS-MG microparticles containing different hydrocortisone loadings were examined
212 with SEM imaging as shown in Figure 2. The rough morphology of these microparticles is thought to
213 result from polymer phase separation at the surface of the drying droplets ^[24].

214 INSERT Table 1

215 INSERT Figure 2

216 Powders prepared from AQOAT AS-MG tended to aggregate. The presence of aggregates increases
217 the voids within the powder bed and results in relatively low tap densities compared with Eudragit
218 L100 microparticles^[24] (Table 1). Further investigation of the pH-responsiveness of these spray dried
219 microparticles, from pH 5 to 7, demonstrated that AQOAT AS-MG particles dissolve at a lower pH
220 than expected, between pH 5.3 and 5.4 (data not shown). Similar observations were reported by
221 Friesen et al who found AQOAT AS-MG soluble above pH 5.2^[25]. In contrast, Eudragit L100
222 microparticles dissolved at pH 5.8 to 5.9, close to the reported polymer solubility threshold of pH 6
223^[24]. Differential scanning calorimetry did not show any changes between the polymer microparticles
224 and the initial AQOAT AS-MG powder (data not shown). The discrepancy in pH-responsiveness
225 between the manufacturer information and experimental results for AQOAT AS-MG might be a
226 result of differences in testing methodologies; the manufacturer's information is based on
227 disintegration testing of 1 cm² polymeric films which may dissolve more slowly than the
228 microparticles^[26].

229 Due to the relatively high drug burst release observed previously with spray-dried Eudragit L100
230 microparticles at pH 5 and 1.2^[24], pHs at which the polymer is not soluble, an alternative
231 microencapsulation technique, namely, the solvent-evaporation method, was investigated.

232 **3.1.2 Oil-in-water emulsification/solvent evaporation technique**

233 In the oil in water emulsification process, the drug and polymer are first dissolved in a water-
234 immiscible solvent, usually dichloromethane (DCM), and the resulting organic phase is emulsified
235 into an aqueous phase containing an appropriate emulsifier. The organic solvent can then be
236 removed by evaporation or extraction. The method has been used to prepare Eudragit-based
237 systems, for the sustained release grades RL and RS^[27, 28], which are neutral copolymers of poly
238 (ethylacrylate, methyl methacrylate) and trimethyl aminoethyl methacrylate chloride^[27]. pH-
239 responsive particles have also been successfully prepared using Eudragit P-4135F^[29-31]; Eudragit P-
240 4135F is synthesised by the co-polymerisation of methacrylic acid, methyl methacrylate and methyl
241 acrylate^[31] and exhibits a dissolution threshold of pH 7.2^[31].

242 The above Eudragit grades are all soluble in DCM, which is advantageous as it facilitates the
243 emulsification of the polymer solution. Moreover, the limited solubility of DCM in water prevents
244 drug loss to the external aqueous phase which can occur with solvent diffusion. However, Eudragit
245 L100 is not soluble in DCM whereas AQOAT AS-MG is only partially soluble (swellable)^[32]. Therefore,
246 a mixed solvent of 7:3 v/v DCM/ethanol was used to solubilise the polymers in the initial organic
247 phase^[33-36], the ethanol content was minimised to limit drug diffusion into the aqueous phase.

248 Using the DCM/ethanol cosolvent system, microparticles were successfully prepared using a 10%
249 w/v AQOAT AS-MG organic solution (Figure 3). The hollow nature of these microparticles is
250 attributed to rapid ethanol diffusion followed by polymer precipitation ^[35]. The rate of solvent
251 diffusion during the initial stage of microparticle preparation is determined by its water solubility.
252 The aqueous solubility of DCM at 25°C is 1.85% ^[2, 11] whereas ethanol is completely miscible with
253 water. The partial solubility of AQOAT AS-MG in DCM means that the polymer shell formed at the
254 interface of the emulsification droplets is non-rigid. This allows for DCM evaporation through
255 eruptions in the polymeric shell. The net result is the formation of spherical intact microparticles
256 with a porous surface upon complete shell solidification (e.g. Figure 3, D).

257 INSERT Figure 3

258 These morphological observations are consistent with tap density measurements of AQOAT AS-MG
259 microparticles (Table 2), which are considerably lower than those calculated for the spray dried
260 powders (Table 1) and are attributed to the hollow nature of the particles. However, hydrocortisone
261 encapsulation into AQOAT AS-MG microparticles resulted in relatively low encapsulation efficiencies
262 (Table 2) probably as a result of rapid ethanol flux into the external aqueous phase. A comparable
263 phenomenon was reported in the literature for the encapsulation of estradiol and indometacin into
264 Eudragit L100-55 ^[6].

265 INSERT Table 2

266 Although hydrocortisone is a hydrophobic drug, it exhibits an appreciable solubility in aqueous
267 media of 0.28 mg/ml ^[16]. The diffusion of ethanol into the external aqueous phase during the
268 emulsification process leads to drug leaching and increased hydrocortisone solubility in the external
269 aqueous phase. This phenomenon may explain the low encapsulation efficiency measured and the
270 appearance of drug crystals in the external aqueous phase at 25% w/w theoretical drug loading
271 (Figure 3, C). Microparticles prepared at 2.5% w/w drug loading show similar morphological
272 characteristics to the drug-free microparticles with no visual evidence of drug crystallisation (Figure
273 3, B). Nonetheless, the encapsulation efficiency of the drug was low despite the fact that it was
274 incorporated at a level well below its solubility limit within the polymer.

275 In contrast, at 10% w/w polymer concentration, sticky Eudragit L100 droplets were produced during
276 the early stages of the oil-in-water emulsification process leading to the formation of elongated
277 polymeric structures (data not shown). In an attempt to overcome this problem, a reduced polymer
278 concentration was used to decrease polymer-polymer interactions in the initial polymeric organic
279 solution which, in turn, reduces the polymer's tendency for precipitation and enables polymer

280 emulsification into the external aqueous phase. Nonetheless, the emulsified droplets generated in
281 the early stages of particle formation tended to collapse during the solvent evaporation step (Figure
282 3, E), possibly due to the brittle nature of the Eudragit L100 shell that forms at the interface of the
283 droplets. The glass transition temperature of Eudragit L100 was reported to be about 160°C with a
284 corresponding minimum film formation temperature (MFT) of 85°C [36]. Similarly to AQOAT AS-MG,
285 the hollow nature of Eudragit L100 microparticles is attributed to rapid ethanol diffusion, polymer
286 precipitation and subsequent shell formation.

287 **3.2 Oil-in-oil emulsification/solvent evaporation technique**

288 An oil-in-oil emulsification process was adopted to circumvent the problem of drug leakage into the
289 external phase. Kendall et al have recently developed a reproducible oil-in-oil microencapsulation
290 method for fabricating Eudragit L100 microparticles intended for gastrointestinal delivery [19]. The
291 method uses liquid paraffin, a non-solvent for both drug and polymer, as the external oil phase.
292 Despite the fact that the use of DCM (ICH class 2) was avoided and ethanol (ICH class 1) was chosen
293 to solubilise the polymer in the internal oil phase, the utilisation of hexane (ICH class 2) for external
294 oil phase removal is inevitable.

295 Drug-free Eudragit L100 microparticles prepared from a 10 % w/v polymeric solution using the oil-in-
296 oil emulsification process have a smooth surface and are less polydisperse than microparticles
297 produced from the spray drying method (Figure 4) with no observed surface porosity. The
298 solubilisation of 2.5% and 10% w/w hydrocortisone in the initial polymeric solution led to the
299 formation of spherical microparticles with similar morphological characteristics. At 25% w/w
300 theoretical drug loading, hydrocortisone was not fully soluble in the initial polymeric solution due to
301 its limited solubility in ethanol. Therefore, the non-solubilised drug crystals are incorporated into
302 relatively large microparticles (about 150 µm diameter compared with 30 µm diameter for drug-
303 free, 2.5 and 10% drug-loaded microparticles) (Figure 4). The presence of drug crystals at a relatively
304 high theoretical loading might have increased the viscosity of the initial polymeric solution. A more
305 viscous phase will require larger shear stress (stirring in this case) to break the emulsion droplets
306 into smaller sizes.

307 INSERT Figure 4

308 Yield, encapsulation efficiency and tap density results obtained from the emulsification of 10% w/v
309 polymeric solutions into liquid paraffin are presented in Table 3. The encapsulation efficiencies
310 obtained for hydrocortisone are relatively high, comparable to those calculated for the spray dried
311 powders (Table 1). The lower encapsulation efficiency at 25% w/w theoretical drug loading can be

312 explained by the loss of uncoated drug crystals into the external oil phase. The high tap density
313 measurements obtained for the oil in oil microparticles suggest that they are solid. However, the oil-
314 in-oil generated Eudragit L100 microparticles with 25% hydrocortisone-loading presents a low tap
315 density due to the presence of crystals within the microparticles which might have disturbed their
316 internal structure and led to pore formation (Figure 4, D).

317 INSERT Table 3

318 The relatively high polymer concentration (10 % w/v), used in the internal oily phase, increased
319 polymer viscosity and caused rapid droplet solidification ^[2]. The rapid solidification of microparticles
320 is advantageous in achieving high drug encapsulation efficiency as it hinders drug migration to the
321 particles' surface ^[2]. In fact, a 1% w/v Eudragit L100 concentration led to inefficient hydrocortisone
322 encapsulation with apparent drug crystals in the external phase and on the surface of the dried
323 microparticles (data not shown). In this case, the low polymer viscosity and slow droplet
324 solidification allowed more time for drug loss through diffusion.

325 The transferability of the oil-in-oil microencapsulation method to different grades of Eudragit; L100,
326 S100 and L55, has been reported by Kendal et al. ^[19]. Nonetheless, its applicability to structurally
327 non-related polymers has not been investigated. Here, the oil-in-oil emulsification method was used
328 to prepare AQOAT AS-MG microparticles but the initial oil phase was substituted by a 7:3 v/v
329 DCM/ethanol co-solvent system to allow for AQOAT solubilisation. SEM images of the obtained
330 microparticles show similar morphological characteristics to Eudragit L100 particles but with a
331 rougher surface topography (Figure 4, E and F).

332 Unlike the oil-in-water emulsification method, the microparticles obtained from the oil-in-oil
333 microencapsulation process appear to be solid. This can be attributed to the relatively slow “good
334 solvent” (ethanol) removal rate. This allows time for polymer redistribution within the drying
335 droplets and results in the formation of solid microparticles. Even when a mixed solvent of
336 DCM/ethanol is used, as for AQOAT AS-MG, the morphology of the particles obtained is similar to
337 that for Eudragit using ethanol alone.

338 **3.3 Drug release**

339 From the different microencapsulation techniques tested, spray drying and the oil-in-oil
340 microencapsulation method resulted in the successful formation of microparticles with efficient drug
341 encapsulation. Dissolution data of these powders are in Figure 5, showing stepped dissolution of
342 microparticles below and above the pH solubility of the polymer. Although the size of the
343 microparticles can influence the rate of drug release in the initial stages, here we compare total drug

344 release after 2 hours at pH 5, when a plateau is reached. Total drug release at this stage is more
345 likely to be due to other factors such as particles porosity or drug distribution. In fact, a study that
346 investigated the release 5-fluorouracil-loaded PLGA-based microparticles has showed that
347 underlying drug release mechanisms were independent of the microparticle size ^[37]. Although the
348 different size fractions released the drug at different rates initially, they all reached the same level of
349 relative drug release after 21 days ^[37].

350 INSERT Figure 5

351 With both preparation methods, Eudragit L100 microparticles showed better controlled release
352 properties than ACOAT AS-MG microparticles, i.e. lower relative drug release after 2 hours at pH 5.
353 At 2.5% and 10% w/w hydrocortisone-loading, Eudragit L100 microparticles obtained from the oil-in-
354 oil encapsulation technique led to negligible hydrocortisone release at pH 5 (Figure 5, B). At 25%
355 w/w drug loading, due to the limited solubility of hydrocortisone in ethanol (11.4 ± 0.33 mg/ml),
356 about 50% of the drug was not dissolved in the initial polymeric solution. During the emulsification
357 process, the non-dissolved drug crystals preferentially distribute on the particles' surface (Figure 4,
358 D) resulting in about 40% drug burst release at pH 5 after 2 hours (Figure 5, B). This suggests that the
359 remaining 10% of undissolved drug crystals is incorporated deeper into the polymer matrix. In
360 contrast, regardless of the drug loading level, the spray dried powders showed a high burst release
361 effect at pH 5, a pH at which the polymer is not soluble (Figure 5, A).

362 These variations in drug release can be attributed to differences in microparticle formation during
363 manufacture. The burst release observed from the spray-dried microparticles implies that they are
364 porous; the presence of pores within microparticles leads to rapid water penetration inside the
365 particles and subsequent rapid diffusion of the encapsulated drug. The process of pore formation
366 during spray drying arises from phase separation during the encapsulation process and subsequent
367 drug partitioning between polymer-poor and rich regions within the drying droplet ^[24]. This
368 phenomenon results in some drug entrapped within the polymer-poor region which dries to form
369 pores or less supported structures ^[11].

370 Interestingly, the spray dried microparticles containing hydrocortisone below the solubility limit
371 within the polymer (2.5 and 10% w/w) provided lower burst release than at 25% w/w loading (Figure
372 5, A). Spray drying below the solubility limit of the drug might lead to higher drug content in the
373 polymer-rich regions of the dried particles and possibly better controlled release properties.
374 Nonetheless, at 2.5% and 10% w/w hydrocortisone loading, the burst release at pH 5 was only
375 reduced by about 10% at 2 hours compared to that when the drug exceeded its solubility at 25%

376 w/w load. This implies that either; a) drug partitioning to polymer-poor regions was still
377 predominant or b) drug enrichment at the surface was also accounting for the drug burst release. As
378 the evaporating droplet shrinks, its receding droplet surface leads to increased solute concentration
379 at the surface and subsequent diffusional flux to the centre ^[38]. During the spray drying process, high
380 solvent evaporation rates can lead to rapid droplet shrinking which does not allow time for drug
381 redistribution and results in surface drug enrichment ^[14].

382 On the other hand, with the oil-in-oil microencapsulation process, solvent evaporation occurs more
383 slowly as the emulsified droplets are stirred overnight at room temperature to allow for complete
384 solvent evaporation. The relatively long evaporation time during the oil-in-oil microencapsulation
385 process, compared with the fast solvent evaporation during spray drying, allows adequate time for
386 both drug and polymer redistribution and diffusion to the centre of the emulsified droplets which
387 may result in better controlled release characteristics. Moreover, the long evaporation time is less
388 likely to produce porous microparticles. In comparison to Eudragit L100 microparticles,
389 hydrocortisone-loaded AQOAT AS-MG particles resulted in a significantly higher drug release at pH 5
390 (Figure 5, C & D) despite the fact that the drug was incorporated at 2.5% w/w, a level well below the
391 solubility limit of hydrocortisone within the polymer matrix. This can be attributed to differences in
392 the internal phase solvent system. The use of a DCM/ethanol co-solvent system may lead to a more
393 porous structure due to the relatively fast evaporation of DCM and might explain the lower tap
394 density measurements obtained for AQOAT AS-MG microparticles (Table 2).

395 It is notable that the rate of drug release from the oil in oil microparticles at pH 7 (Figure 5, B, post
396 120 mins) increases with drug loading. This effect may reflect drug distribution within the polymer
397 matrix; the more drug available at or near the surface of the particle the more rapid is the initial
398 release since less polymer is available to hinder drug diffusion. Using the same oil in oil
399 microencapsulation method, Nilkumhang et al. investigated partitioning of fluorescent dyes
400 between the internal (ethanol) and external (liquid paraffin) phases and found a correlation between
401 the partition coefficient and molecular distribution within the prepared microparticles ^[39]. However,
402 in this study, the same drug is used and the partition coefficient between ethanol and liquid paraffin
403 is therefore constant.

404 **3.4 Mechanisms of “burst release”**

405 **3.4.1 Particle density and percentage porosity**

406 Wang and Wang (2002) suggested that the density of the produced microparticles could profoundly
407 influence drug release since increased particulate density can restrict the diffusion of the drug from

408 the microparticles^[11]. Tap density measurements can offer insight into this phenomenon; assuming
409 perfect packing of the tapped powder and a monodisperse size distribution, tap density values are
410 approximately a 21% underestimate of particle density^[40]. Although this method may not fully
411 discriminate between subtle structural differences due to possible electrostatic interactions,
412 especially when dealing with small particles, it has previously been useful employed to study
413 microparticles^[20] and the data supports that from our SEM imaging and Raman microscopy
414 investigations.

415 Tap density measurements of the spray dried and oil-in-oil microparticles are reported in Table 1
416 and 3 respectively. For both polymers loaded with drug below the solubility limit (2.5% and 10%
417 w/w), the oil-in-oil microparticles displayed significantly higher tap densities than the spray dried
418 particles. This correlates with *in-vitro* release testing as the more dense oil-in-oil Eudragit particles
419 showed negligible drug release at pH 5 (Figure 5, B) compared with the less dense spray dried
420 particles of the same polymer (Figure 5, A). Likewise, the oil-in-oil generated AQOAT particles gave
421 lower burst release at pH 5 than the equivalent spray dried material. Thus, for both polymers,
422 significant burst release correlated with lower tap densities.

423 In contrast, microparticles prepared from the oil/oil method at 25% w/w drug-loading showed a
424 significantly lower tap density measurement than other Eudragit L100 microparticles (Table 3)
425 suggesting a higher level of intraparticulate voids ($p < 0.05$). This increased porosity might be due to
426 the presence of drug crystals in the initial polymeric solution which might have disturbed the flow of
427 the polymer within the emulsification droplets leading to the formation of pores. Moreover, drug
428 crystals are more likely to accumulate at the polymer/liquid paraffin interface during droplet drying
429 and surface recession. Eudragit S100 microparticles containing 50% and 66.7% w/w prednisolone
430 were hollow and showed an extensive amount of crystalline drug on the surface^[41]. As expected,
431 these morphological changes were also attributed to a high burst release^[41]. Similarly, Yadav et al.
432 (2009)^[42] showed that increased intraparticle porosity of carbamazepine in Eudragit RSPO was due
433 to low polymer deposition in the empty spaces between the agglomerated microcrystals. Increased
434 drug deposition at the surface of our microparticles coupled with increased intraparticulate porosity
435 explains the relatively high burst release of hydrocortisone from 25% w/w drug-loaded
436 microparticles produced from the oil in oil emulsification method (Figure 5, B).

437 **3.4.2 Residual solvent level**

438 Burst release of rifampicin from poly(D, L-lactic acid) (PDLLA)/ Resomer (30:70) spray dried
439 microparticles was attributed to residual solvent reducing the glass transition temperature (T_g) of
440 the polymer, leading to accelerated water uptake and greater drug diffusion from the microparticles

441 ^[13]. The residual solvent in the microparticles prepared from the oil-in-oil and spray drying methods
442 at different drug loadings was determined using thermo-gravimetric analysis (Table 4). No significant
443 differences ($P>0.05$) were seen between the two methods of manufacture or between various drug
444 loadings, showing that, for these particles, residual solvent effects were not responsible for burst
445 effects. It should be noted that residual paraffin from the oil in oil method is not detected by this
446 technique. However, paraffin is a hydrophobic non-solvent for the polymer and therefore is not
447 expected to increase water uptake or influence drug release.

448 INSERT Table 4

449 3.4.3 Drug crystallinity

450 Differential scanning calorimetry and X-ray analysis of Eudragit L100, hydrocortisone, drug-free
451 microparticles and hydrocortisone-loaded microparticles were used to identify changes in drug form
452 that might have occurred during the encapsulation process (Figures 6 and 7). Drug encapsulation
453 within microparticles depends on its initial state in the polymeric solution and on the preparation
454 process ^[43]. Differential scanning calorimetry of untreated Eudragit L100 shows a broad phase
455 transition between 180 and 235°C (Figure 6). The nature of this phase transition is still unclear, but
456 dissociation of inter-molecular hydrogen bonds and anhydride formation has been suggested ^[44].
457 The DSC curve of hydrocortisone powder show an endothermic melting peak at $222\pm 0.7^\circ\text{C}$ (Figure 6),
458 in accordance with the literature value of $221\pm 2^\circ\text{C}$ ^[45].

459 INSERT Figure 6

460 INSERT Figure 7

461 Drug-free, 2.5% and 10% w/w hydrocortisone-loaded Eudragit L100 microparticles prepared from
462 the oil-in-oil microencapsulation method did not show any additional phase transitions to those
463 already observed in the untreated Eudragit powder. This suggests that, at 2.5% and 10%
464 hydrocortisone loading, the drug is soluble in the Eudragit L100 polymer matrix giving rise to a solid
465 solution. For 25% hydrocortisone-loaded microparticles, where a proportion of the drug was
466 incorporated in its crystalline form, a small endothermic peak at around 200°C corresponding to
467 melting point depressed hydrocortisone crystals was observed. X-ray analysis of these samples
468 (Figure 7) supports the DSC data with no crystalline drug found at low loadings but excess drug (at
469 25% w/w loading) was present in the same crystalline form as the starting material.

470 However, for spray dried materials, hydrocortisone-loaded Eudragit L100 microparticles show an
471 endothermic shoulder which moves to a lower temperature as the drug loading increases (Figure 6).
472 However, as the polymer also shows an endothermic peak in the same region, it was unclear

473 whether this thermal feature was due to the presence of drug crystals. From the X-ray diffraction
474 patterns of unprocessed drug and hydrocortisone-loaded microparticles, the intense crystalline
475 peaks at 14.5 and 17 degrees 2θ , observed for unprocessed hydrocortisone, were absent in the
476 diffractogram of drug-containing spray dried microparticles (Figure 7). This suggests that the drug is
477 present in an amorphous form within the spray dried microparticles. The presence of amorphous
478 drug, coupled with the small size of spray dried microparticles may facilitate drug release and can
479 partly explain the relatively high burst release observed for this material (Figure 5, A). However, the
480 fact that the drug is non-crystalline at 2.5% and 10% w/w within Eudragit L100 microparticles
481 produced from the oil-in-oil microencapsulation method suggests that this phenomenon is not solely
482 responsible for the non-controlled burst effect; a further potential mechanism is the relatively high
483 drug enrichment at the surface of the spray dried microparticles compared with the oil-in-oil
484 powders.

485 **3.4.4 Drug distribution within the microparticles**

486 In order to clarify whether release from the microparticles relates to the spatial distribution of the
487 drug within the polymer matrix, confocal Raman microscopy was used for depth profiling Eudragit
488 L100 microparticles^[46]. As discussed above, the evaporation of ethanol during microencapsulation
489 can result in drug migration to the microparticle's surface resulting in surface drug enrichment which
490 can result in a higher or more rapid drug release.

491 Figure 8 shows the Raman spectra of hydrocortisone and Eudragit L100 powders used for
492 microparticle production. Hydrocortisone has characteristic Raman bands at 1643 and 1610 cm^{-1}
493 which are consistent with C=C stretching modes at the 4-5 position^[47, 48] (Figure 8). On the other
494 hand, Eudragit L100 shows distinctive Raman peaks at 1751 and 1451 cm^{-1} which are assigned to the
495 C=O stretching and $-\text{CH}_2-$ scissoring modes respectively^[48]. The Raman spectrum of this polymer
496 also displays relatively strong peaks at 1205, 1120, 969 and 812 cm^{-1} which are associated with C-H
497 and C-C wagging vibrations^[48].

498 Insert Figure 8

499 Raman depth profiling of Eudragit L100 microparticles at 25% w/w drug-loading is shown in Figure 9,
500 A (data not shown for 2.5% and 10% w/w drug-loading). Based on the linear relationship between
501 the intensity of the peak from the measured analyte and its concentration^[49], the depth profiles
502 were processed to acquire component graphs detailing the proportion of both hydrocortisone and
503 Eudragit L100 as a function of depth (Figure 9, C, D and E). At 25% w/w drug-loading, the intensities
504 of the characteristic hydrocortisone peaks at 1643 and 1610 cm^{-1} were variable: they increased
505 dramatically at a depth of 12 μm then declined (Figure 9, A). This high intensity region coincides with

506 the presence of a drug crystal inside the microparticle as illustrated in the SEM image of a
507 microtomed 25% w/w hydrocortisone-loaded particle where drug crystals can be seen both on the
508 surface and within the polymer matrix (Figure 9, B). It should also be noted that this SEM image
509 supports tap density measurements obtained for the 25% w/w drug-loaded microparticles (Table 3).
510 The considerably lower tap density measurement of these microparticles (Table 3) compared to
511 other powders containing lower amounts of drug is due to a higher level of intraparticulate voids.
512 SEM images of the internal structure of 2.5% and 10% w/w hydrocortisone-containing microparticles
513 showed no evidence of crystal inclusions.

514 Insert Figure 9

515 In the case of 2.5% and 10% w/w hydrocortisone-loading, the proportion of both hydrocortisone and
516 Eudragit L100 remained constant throughout the depth studied (Figure 9, D and E). Assuming that
517 these microparticles have a monodisperse size of about 30 μm (Figure 4), these results show that the
518 concentration of hydrocortisone at the surface and the core (15.20 μm) is the same, i.e. the oil-in-oil
519 microencapsulation process did not result in drug enrichment on the surface. In contrast, with 25%
520 w/w hydrocortisone-loading, the proportion of hydrocortisone relative to Eudragit L100 varied
521 depending on the presence of drug crystals within the polymer matrix (Figure 9, C). These results
522 support SEM images and XRPD/DSC data, with regions within the particle showing increased
523 intensities of hydrocortisone characteristic bands showing the presence of drug crystals. It should be
524 noted that the data presented in Figure 9 is representative of three different microparticles selected
525 randomly for each drug loading. Unfortunately, depth profiling of the spray dried microparticles for
526 comparative purposes was not possible due to their small particle size (size range 1-5 μm , Figure 2).

527 Since Raman depth profiling of the oil-in-oil microparticles demonstrated that, at 2.5% and 10% w/w
528 drug-loading, no differences in the spatial distribution of hydrocortisone existed within the polymer
529 matrix, variations in drug release at pH 7 can be solely due to differences in the polymer/drug ratio.
530 In other words, an increase in the proportion of Eudragit L100 relative to hydrocortisone, e.g. at
531 2.5% drug-loading, leads to a moderately slower drug release as a larger amount of polymer is
532 available to hinder drug diffusion.

533 **4 Conclusion**

534 Of the different microencapsulation techniques tested, spray drying and the oil-in-oil emulsification
535 method successfully formed microparticles with high levels of drug encapsulation. Scanning electron
536 microscopy and dissolution testing revealed that the microparticles prepared from the oil-in-oil
537 encapsulation method had more favourable morphological and release characteristics. In fact, the

538 encapsulation of hydrocortisone at levels below its saturation solubility within Eudragit L100; 2.5 and
539 10% w/w, lead to negligible release at pH 5, a pH at which the polymer is not soluble, whereas
540 increasing the pH to 7 resulted in near instantaneous drug release. The spray dried powders, on the
541 other hand, showed high drug burst release at pH 5. These variations in drug release are partially
542 attributed to differences in microparticle formation. In contrast with the spray drying process, slow
543 solvent evaporation and droplet solidification during the oil-in-oil emulsification process allows
544 adequate time for drug and polymer redistribution which may result in denser microparticles and
545 better controlled release characteristics. Tap density measurements showed good correlation with
546 *in-vitro* drug release testing and SEM imaging, especially for the oil-in-oil produced microparticles,
547 with high density particles showing better controlled release properties. Thermal, X-ray and
548 confocal Raman analysis of the particles also demonstrates the importance of drug loading on
549 release properties; below the solubility limit, drug was homogeneously distributed and was non-
550 crystalline whereas exceeding the solubility generated crystalline domains in oil-in-oil generated
551 materials with consequent burst release. Thus, both the manufacturing method (which influences
552 particle porosity and density) and drug:polymer compatibility and loading (which affect drug form
553 and distribution) are responsible for burst release seen from our particles.

554 **Acknowledgements**

555 The authors thank Stiefel laboratories Ltd, a GSK company, for their financial support through a PhD
556 studentship which facilitated this work.

557

558 **Figure legends**

559 Figure 1. Microscopic examination of hydrocortisone/ AQOAT[®] AS-MG films (at 10x magnification) at;
560 (A) 0%, (B) 9%, (C) 10% and (d) 20% w/w theoretical loading.

561 Figure 2. Scanning electron microscopy images of spray dried microparticles using Eudragit L100 with
562 (A) 0% and (B) 10%, hydrocortisone loading and AQOAT-AS-MG with (C) 0% and (D) 2.5% drug
563 loading.

564 Figure 3. Scanning electron microphotographs of microparticles prepared by the oil in water
565 emulsification solvent evaporation method; (A) , (B) and (C) show AQOAT AS-MG microparticles at
566 0%, 2.5% and 25% hydrocortisone loading respectively. Image D and E shows 2.5% w/w
567 hydrocortisone-loaded AQOAT microparticles at high magnification and drug-free Eudragit L100
568 microparticles respectively.

569 Figure 4. SEM photomicrographs of Eudragit L100 microparticles prepared from the oil-in-oil
570 emulsification process at; (A) 0%, (B) 2.5%, (C) 10% and (D) 25% w/w theoretical hydrocortisone
571 loading with respect to polymer. Images E and F show AQOAT AS-MG microparticles prepared at 0%
572 and 2.5% hydrocortisone loading respectively.

573 Figure 5. Stepped dissolution testing of prepared microparticles with pH change from 5 to 7 after 2
574 hrs; (A) spray dried Eudragit L100 microparticles at different hydrocortisone loadings, (B) Eudragit
575 L100 microparticles prepared using the oil-in-oil microencapsulation method, (C) 2.5%
576 hydrocortisone-loaded AQOAT AS-MG spray dried microparticles and (D) 2.5% hydrocortisone-
577 containing AQOAT AS-MG microparticles obtained from the oil-in-oil technique. HC denotes
578 hydrocortisone. (mean±SD, n=3).

579 Figure 6. DSC thermograms of Eudragit L100 powder, hydrocortisone, drug-free and hydrocortisone-
580 loaded Eudragit L100 microparticles produced from the spray drying and the oil in oil
581 microencapsulation method.

582 Figure 7. X-ray analysis of starting materials (hydrocortisone and Eudragit L100) and hydrocortisone-
583 loaded microparticles prepared from the oil-in-oil encapsulation method and spray drying.

584 Figure 8. Raman spectra of hydrocortisone (black line) and Eudragit L100 (red line).

585 Figure 9. Raman depth profiling (A) and scanning electron microscopy (B) showing the internal
586 composition of 25% w/w hydrocortisone-loaded microparticles prepared from the oil-in-oil
587 microencapsulation technique. (C), (D) and (E) represents the component analysis of hydrocortisone

588 (red line) and Eudragit L100 (blue line) within the oil-in-oil prepared microparticles as a function of
589 depth. Depth profiling was performed from the surface (0 μm) to a depth of -15.2 μm for 2.5% (E)
590 and 10% w/w (D) hydrocortisone-loaded microparticles and -38.0 μm for 25% w/w drug-containing
591 microparticles (C). HC denotes hydrocortisone.

592 **Table legends**

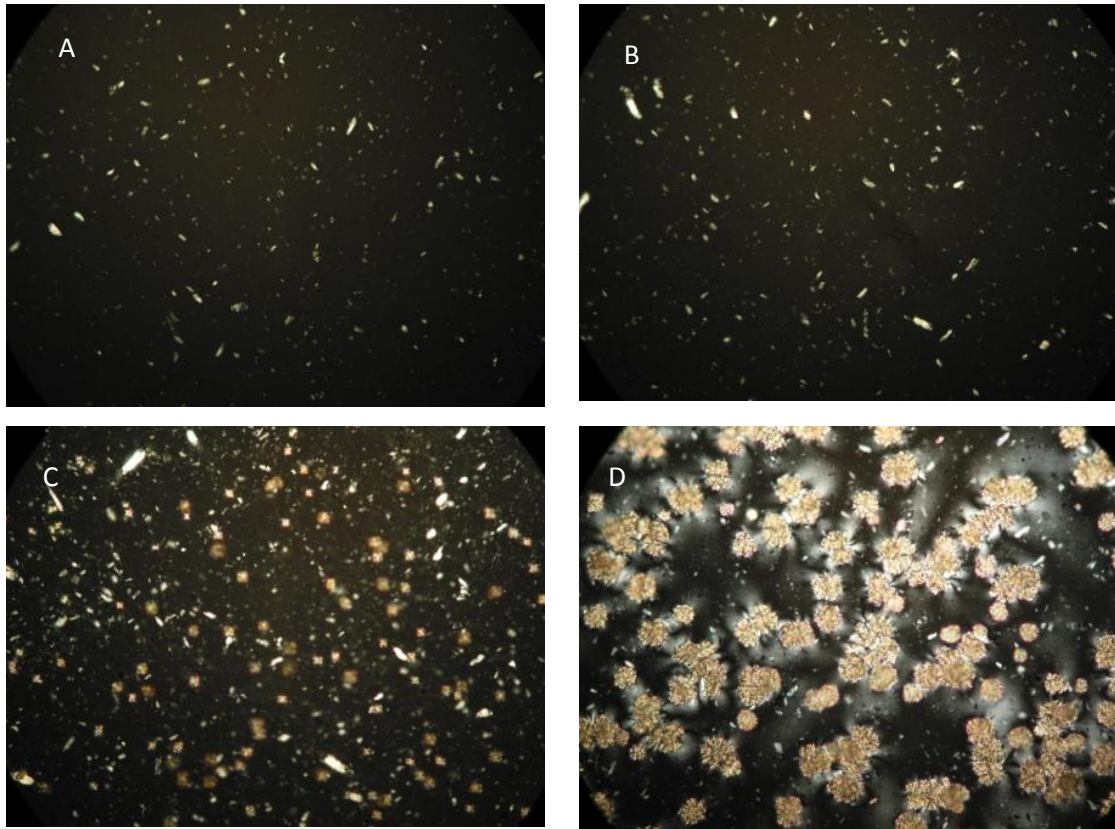
593 Table 1. Yield, tap density and encapsulation efficiency values of Eudragit L100 and AQOAT AS-MG
594 microparticles prepared from the spray drying method with variable hydrocortisone loadings.

595 Table 2. Yield and encapsulation efficiency of hydrocortisone-loaded AQOAT AS-MG microparticles
596 prepared from the oil-in-water emulsification process.

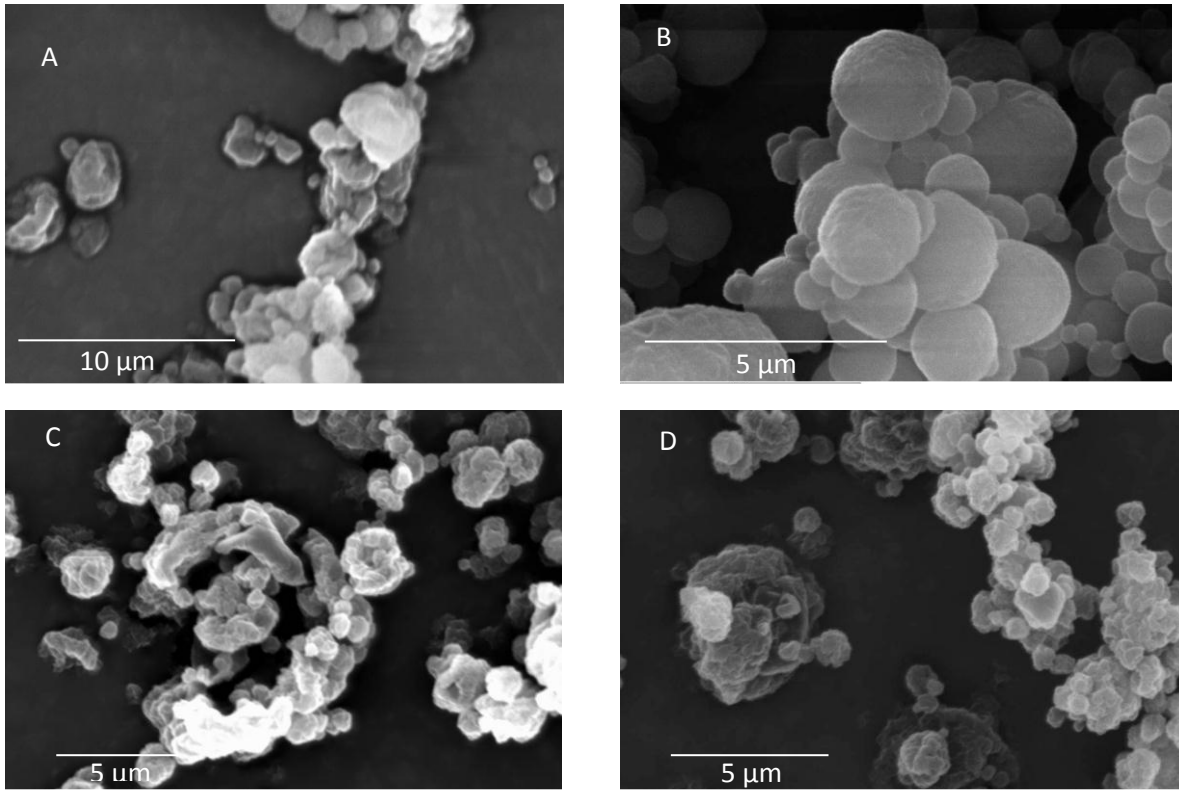
597 Table 3. Yield, tap density and encapsulation efficiency values of Eudragit L100 and AQOAT AS-MG
598 microparticles prepared from the oil in oil emulsification method at variable hydrocortisone
599 loadings.

600 Table 4. Residual solvent content (% w/w) of the microparticles (MPs) prepared from the oil-in-oil
601 and spray drying methods.

602

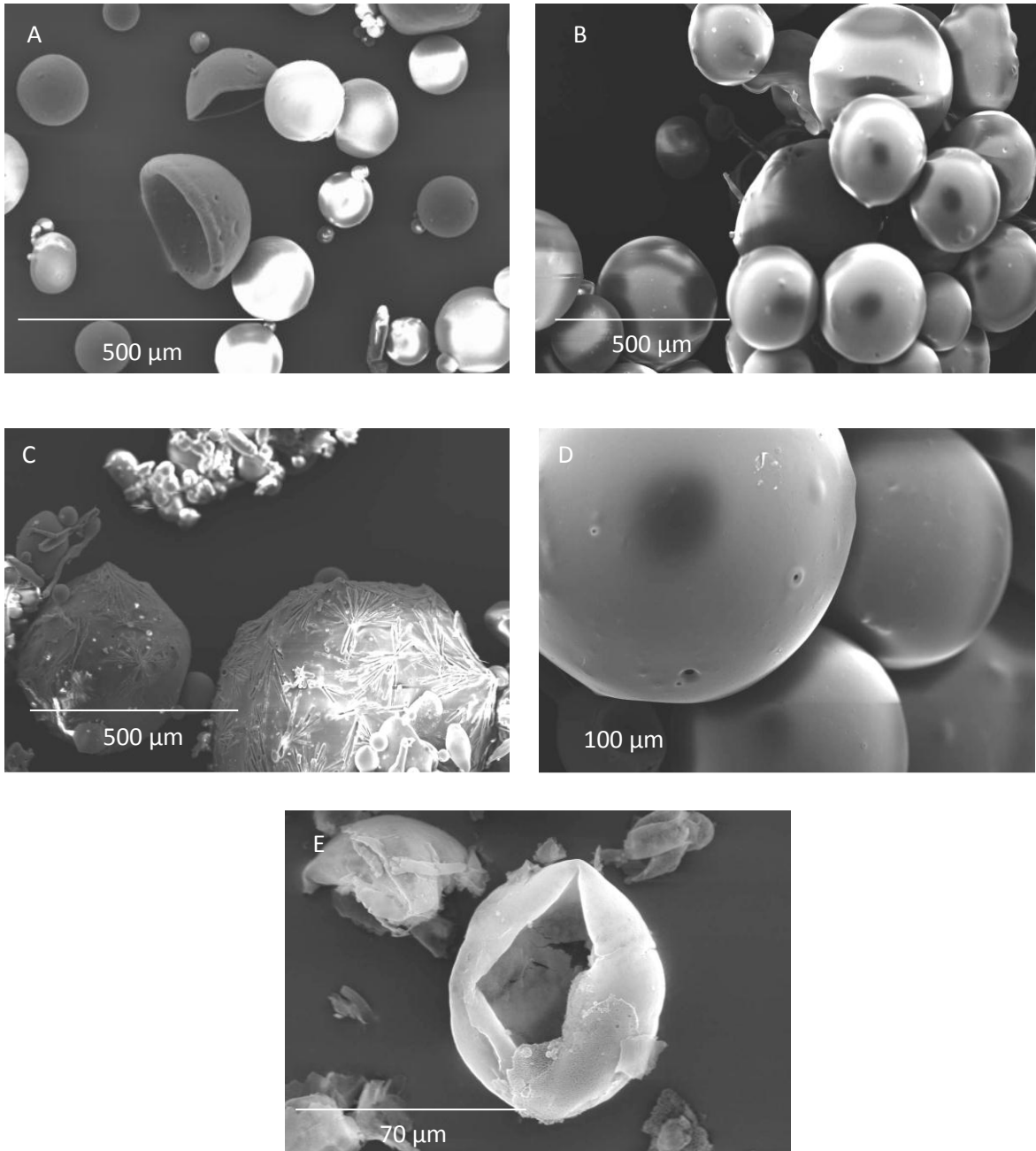


603 Figure 1.. Microscopic examination of hydrocortisone/ AQOAT[®] AS-MG films (at 10x magnification) at; (A) 0%, (B) 9%, (C)
604 10% and (D) 20% w/w theoretical loading.



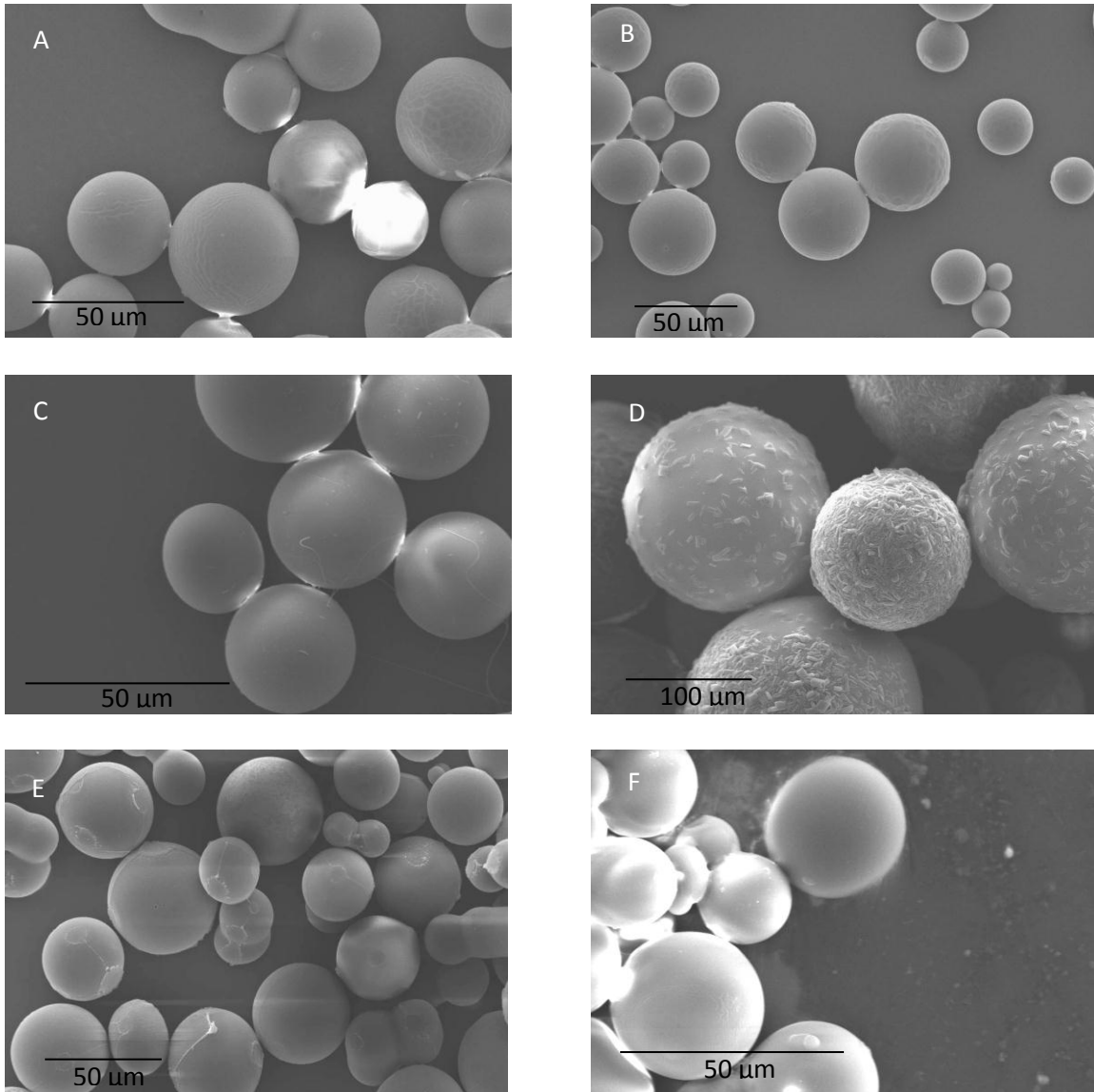
605 **Figure 2. Scanning electron microscopy images of spray dried microparticles using Eudragit L100 with (A) 0% and (B)**
606 **10%, hydrocortisone loading and AQOAT-AS-MG with (C) 0% and (D) 2.5% drug loading.**

607



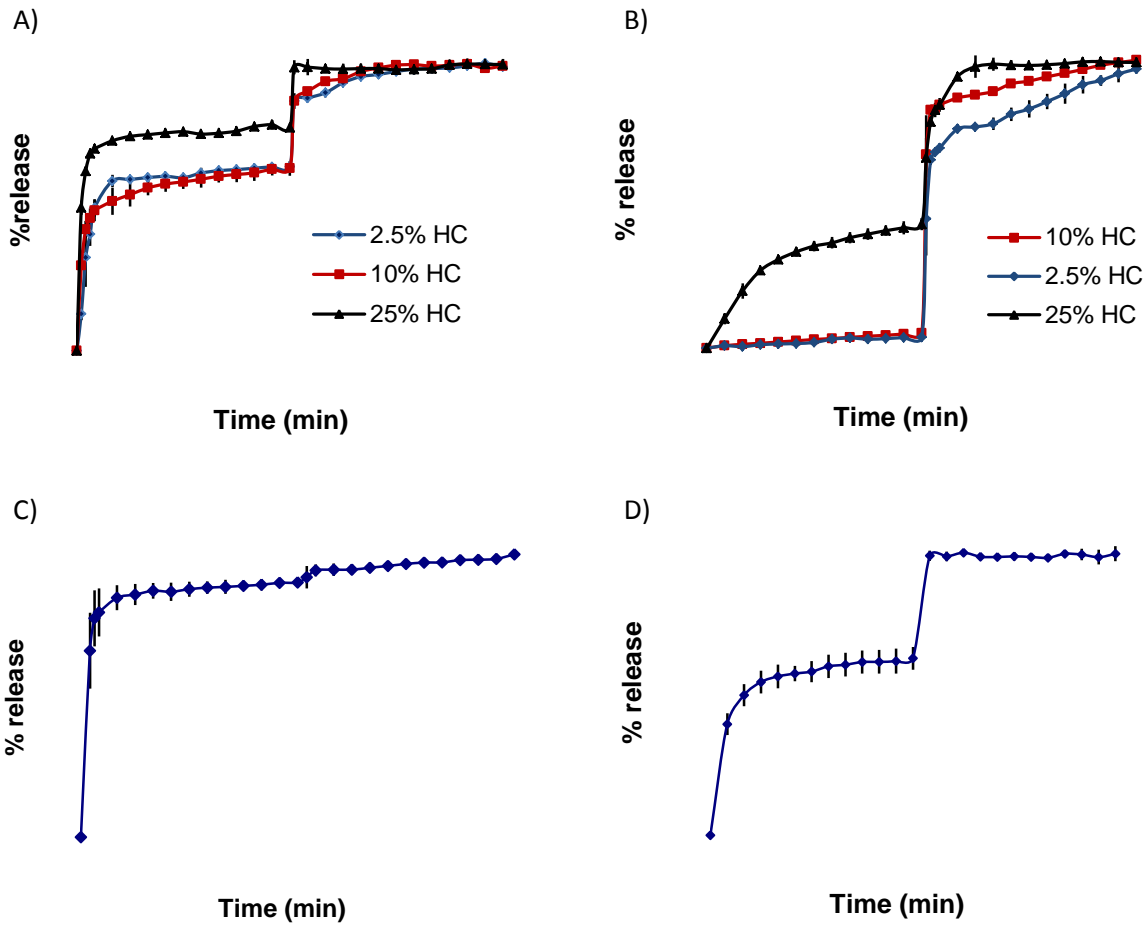
608 **Figure 3. Scanning electron microphotographs of microparticles prepared by the oil in water emulsification solvent**
 609 **evaporation method; (A) , (B) and (C) show AQOAT AS-MG microparticles at 0%, 2.5% and 25% hydrocortisone loading**
 610 **respectively. Image D and E shows 2.5% w/w hydrocortisone-loaded AQOAT microparticles at high magnification and**
 611 **drug-free Eudragit L100 microparticles respectively.**

612



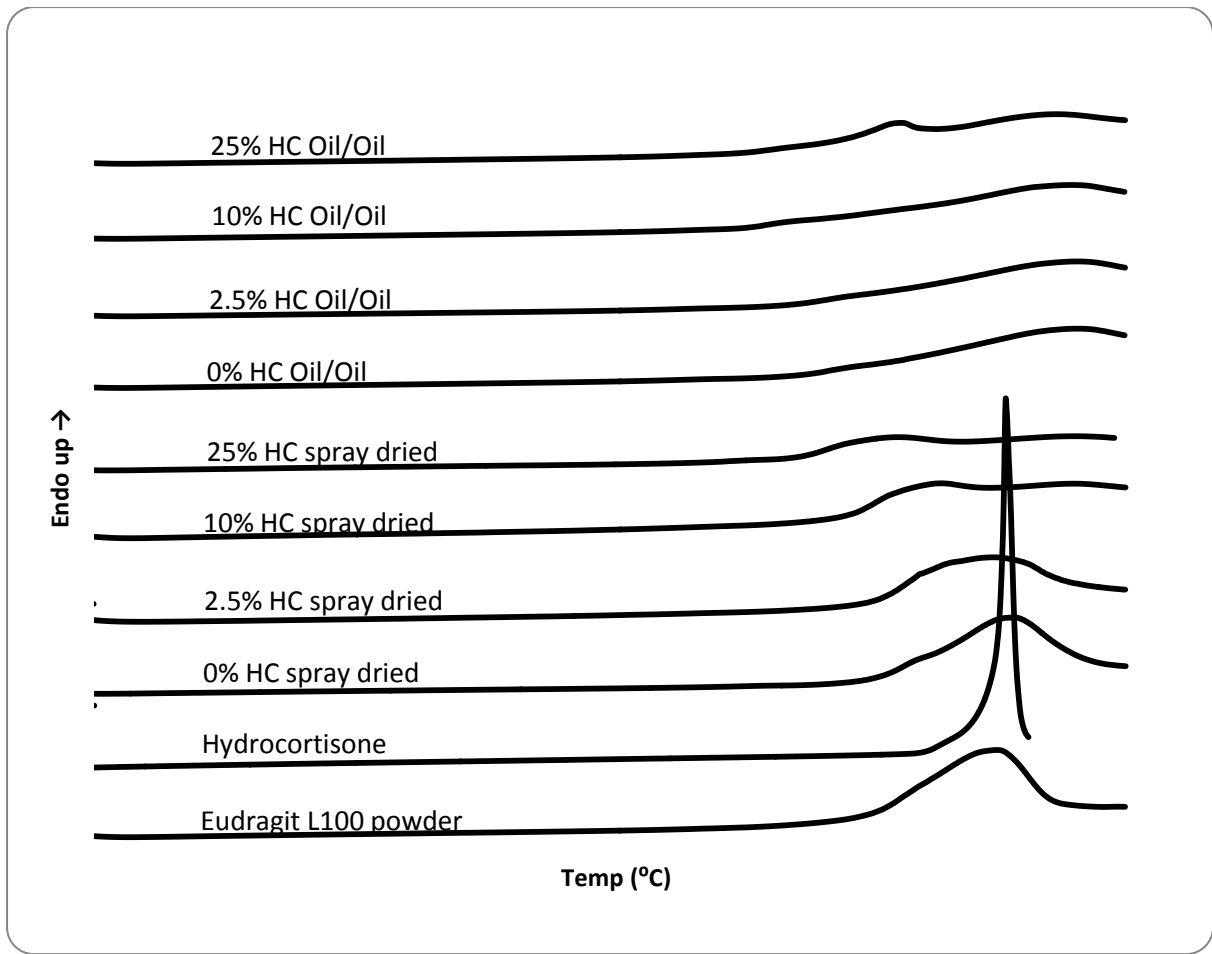
613 **Figure 4. SEM photomicrographs of Eudragit L100 microparticles prepared from the oil-in-oil emulsification process at;**
614 **(A) 0%, (B) 2.5%, (C) 10% and (D) 25% w/w theoretical hydrocortisone loading with respect to polymer. Images E and F**
615 **show AQOAT AS-MG microparticles prepared at 0% and 2.5% hydrocortisone loading respectively.**

616



617 Figure 5. Stepped dissolution testing of prepared microparticles with pH change from 5 to 7 after 2 hrs; (A) spray dried
 618 Eudragit L100 microparticles at different hydrocortisone loadings, (B) Eudragit L100 microparticles prepared using the
 619 oil-in-oil microencapsulation method, (C) 2.5% hydrocortisone-loaded AQOAT AS-MG spray dried microparticles and (D)
 620 2.5% hydrocortisone-containing AQOAT AS-MG microparticles obtained from the oil-in-oil technique. HC denotes
 621 hydrocortisone. (mean \pm SD, n=3).

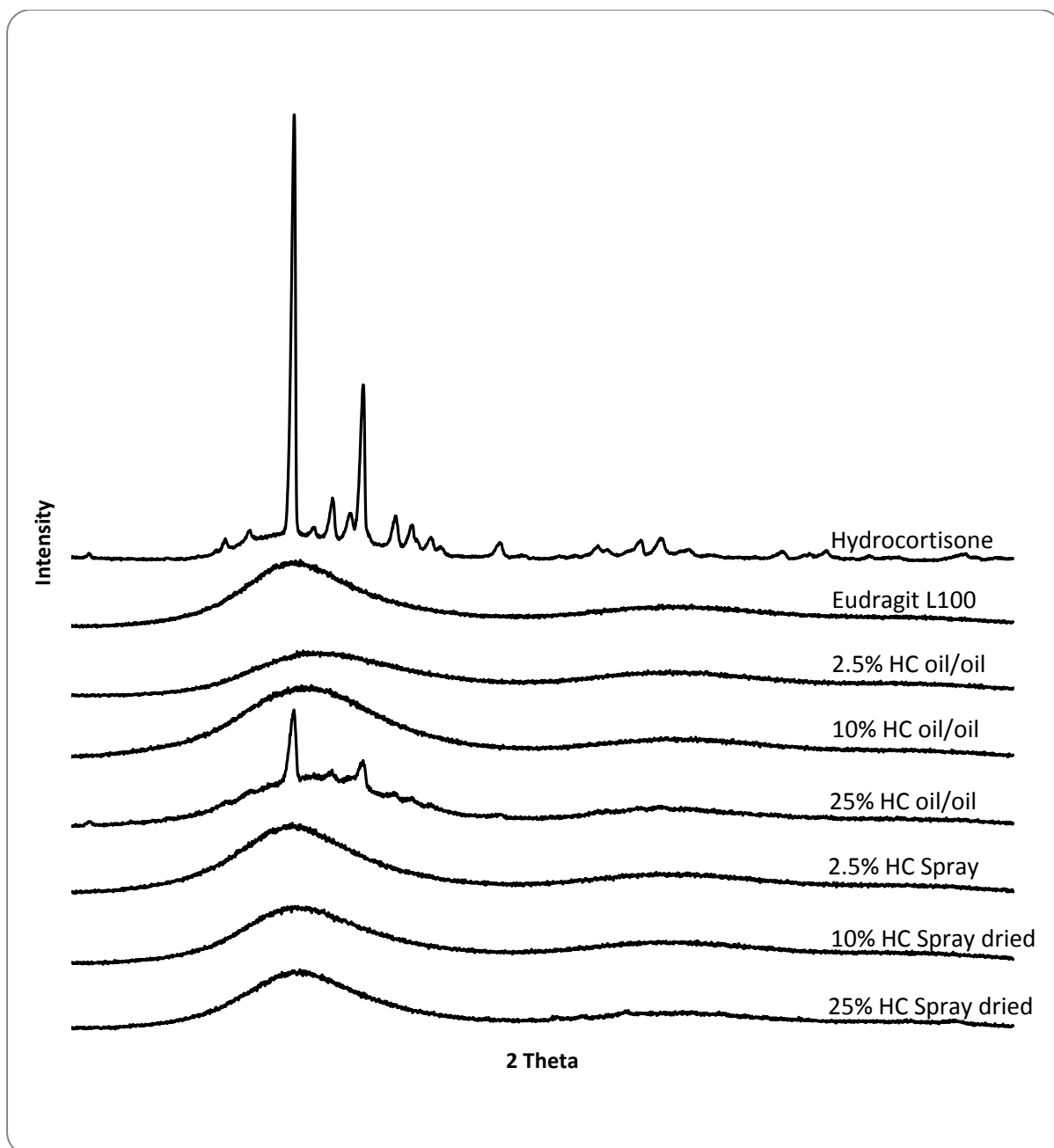
622



623

624 **Figure 6. DSC thermograms of Eudragit L100 powder, hydrocortisone, drug-free and hydrocortisone-loaded Eudragit L100**
 625 **microparticles produced from the spray drying and the oil in oil microencapsulation method.**

626

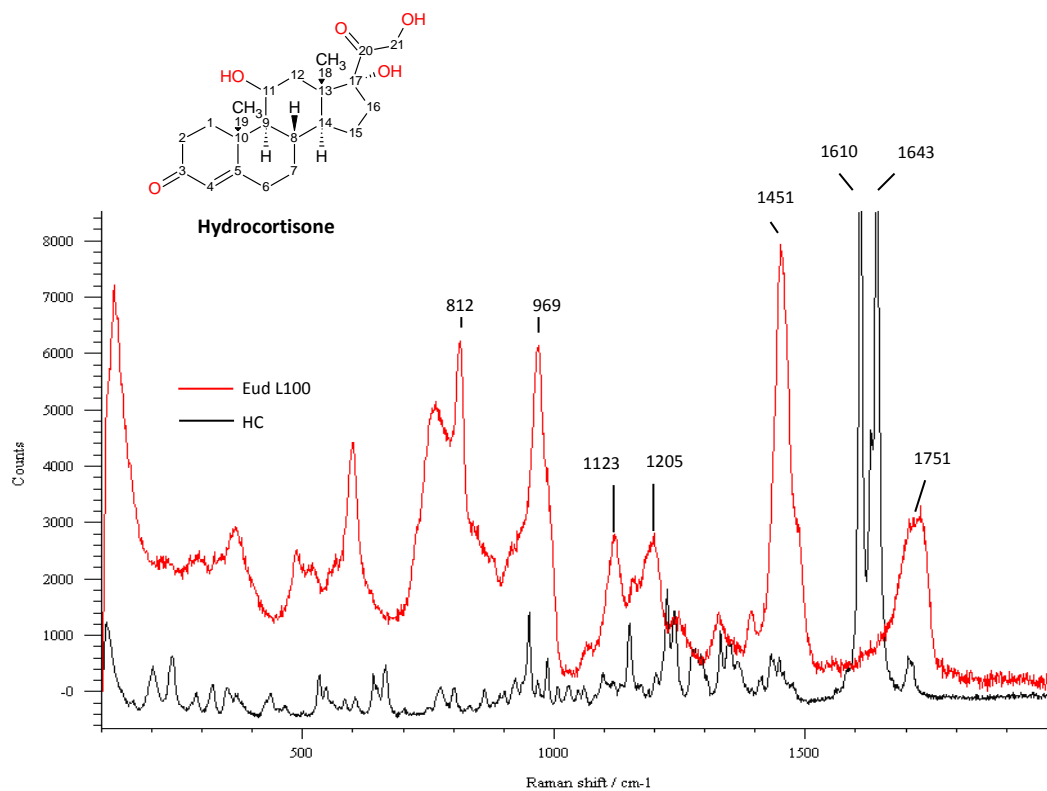


627

628 **Figure 7. X-ray analysis of starting materials (hydrocortisone and Eudragit L100) and hydrocortisone-loaded**
629 **microparticles prepared from the oil-in-oil encapsulation method and spray drying.**

630

631

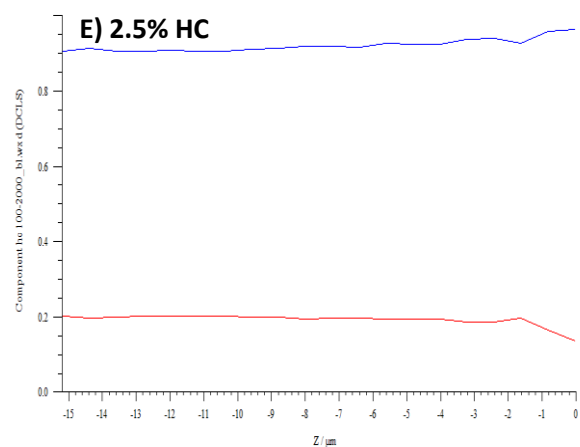
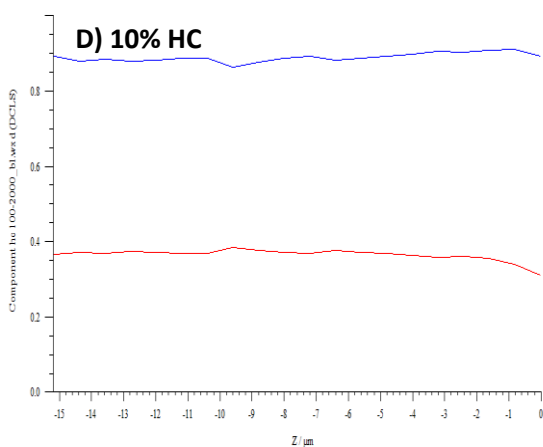
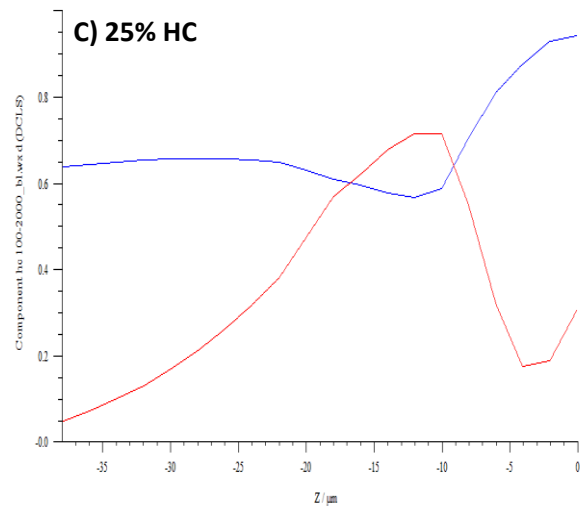
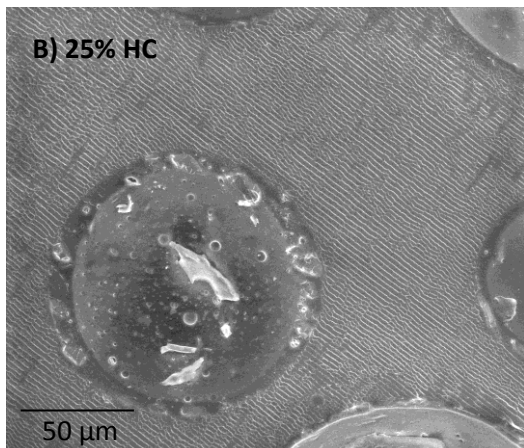
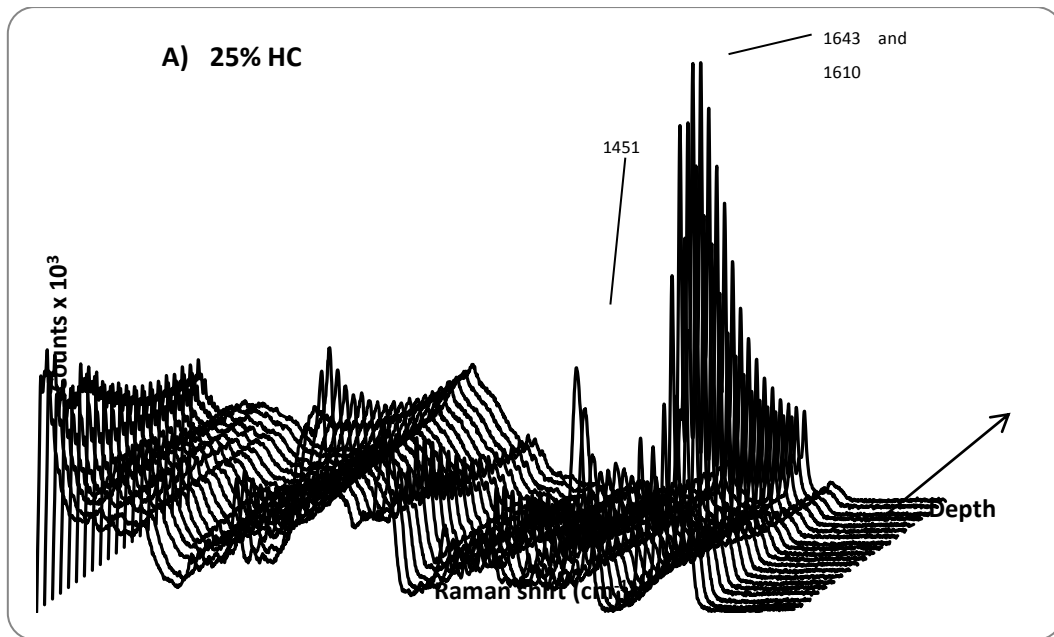


632

633

Figure 8. Raman spectra of hydrocortisone (black line) and Eudragit L100 (red line).

634



635 Figure 9. Raman depth profiling (A) and scanning electron microscopy (B) showing the internal composition of 25% w/w
 636 hydrocortisone-loaded microparticles prepared from the oil-in-oil microencapsulation technique. (C), (D) and (E)
 637 represents the component analysis of hydrocortisone (red line) and Eudragit L100 (blue line) within the oil-in-oil
 638 prepared microparticles as a function of depth. Depth profiling was performed from the surface (0 μm) to a depth of -
 639 15.2 μm for 2.5% (E) and 10% w/w (D) hydrocortisone-loaded microparticles and -38.0 μm for 25% w/w drug-containing
 640 microparticles (C). HC denotes hydrocortisone.
 641

642 **Table 1. Yield, tap density and encapsulation efficiency values of Eudragit L100 and AQOAT AS-MG microparticles**
 643 **prepared by spray drying with variable hydrocortisone loadings.**

Polymer	Drug loading (% w/w)	Yield (%)	Tap density (g/ml)	Encapsulation Efficiency (%)
Eudragit L100	0*	80.6	0.85±0.02	/
Eudragit L100	2.5*	78.7	0.84±0.04	99.1±2.99
Eudragit L100	10	47.7	0.92±0.03	88.6±3.63
Eudragit L100	25*	67.6	1.02±0.01	94.6±1.00
AQOAT AS-MG	0	53.1	0.57±0.03	/
AQOAT AS-MG	2.5	72.7	0.59±0.04	98.9±0.92

644 *Data from Rizi et al. (2010) shown for comparison.

645

646 **Table 2. Yield and encapsulation efficiency of hydrocortisone-loaded AQOAT AS-MG microparticles**
647 **prepared from the oil-in-water emulsification process.**

Drug loading (% w/w)	Yield (%)	Tap density (g/ml)	Encapsulation efficiency (%)
0	88.0	0.31±0.01	NA
2.5	63.2	0.25±0.02	23.35±1.09
25	77.1	0.15±0.01	22.05±1.02

648

649 **Table 3. Yield, tap density and encapsulation efficiency values of Eudragit L100 and AQOAT AS-MG microparticles**
 650 **prepared from the oil-in-oil emulsification method at variable hydrocortisone loadings.**

Polymer	Drug loading (% w/w)	Yield (%)	Tap density (g/ml)	Encapsulation Efficiency (%)
Eudragit L100	0	81.3	0.86±0.05	/
Eudragit L100	2.5	89.5	1.03±0.01	94.84±1.79
Eudragit L100	10	90.7	1.02±0.07	82.04±0.74
Eudragit L100	25	86.0	0.33±0.02	73.62±2.38
AQOAT AS-MG	0	86.7	0.66±0.03	/
AQOAT AS-MG	2.5	90.7	0.86±0.04	100.9±2.9

651

652

653 **Table 4. Residual solvent content (% w/w) of the microparticles (MPs) prepared from the oil-in-oil and spray drying**
654 **methods.**

Hydrocortisone-loading	Spray dried MPs	Oil-in-oil MPs
0%	6.97±0.38	7.74±0.06
2.5%	7.33±1.08	7.64±0.10
10%	7.41±0.56	7.59±0.14
25%	6.59±0.79	7.80±0.38

655

656 5 References

- 657 [1]. Freitas S, Merkle HP, Gander B. Microencapsulation by solvent extraction/evaporation:
658 reviewing the state of the art of microsphere preparation process technology. *J Controlled*
659 *Release*. 2005;102(2):313-332.
- 660 [2]. Wischke C, Schwendeman SP. Principles of encapsulating hydrophobic drugs in PLA/PLGA
661 microparticles. *Int J Pharm*. 2008;364(2):298-327.
- 662 [3]. Pinto Reis C, Neufeld RJ, Ribeiro AJ, Veiga F. Nanoencapsulation I. Methods for preparation
663 of drug-loaded polymeric nanoparticles. *Nanomed Nanotechnol Biol Med*. 2006;2(1):8.
- 664 [4]. Fessi H, Puisieux F, Devissaguet JP. Nanocapsule formation by interfacial polymer deposition
665 following solvent displacement. *Int J Pharm*. 1989;55:R1-R4.
- 666 [5]. Gao Y, Cui F, Guan Y, Yang L, wang Y, Zhang L. Preparation of roxithromycin-polymeric
667 microspheres by the emulsion solvent diffusion method for taste masking. *Int J Pharm*.
668 2006;318:62-69.
- 669 [6]. Dong W, Bodmeier R. Encapsulation of lipophilic drugs within enteric microparticles by a
670 novel coacervation method. *Int J Pharm*. 2006;326(1-2):128.
- 671 [7]. Bodmeier R, Chen H. Preparation of biodegradable poly(\pm) lactide microparticles using a
672 spray-drying technique. *J Pharm Pharmacol*. 1988;40(11):754-757.
- 673 [8]. Palmieri G, Bonacucina G, Di Martino P, Martelli S. Spray-drying as a method for
674 microparticulate controlled release systems preparation: Advantages and limits. I. Water-
675 soluble drugs. *Drug Dev Ind Pharm*. 2001;27(3):195.
- 676 [9]. Hegazy N, Demirel M, Yazan Y. Preparation and in vitro evaluation of pyridostigmine
677 bromide microparticles. *Int J Pharm*. 2002;242(1-2):171.
- 678 [10]. Xu J, Bovet LL, Zhao K. Taste masking microspheres for orally disintegrating tablets. *Int J*
679 *Pharm*. 2008;359(1-2):63-69.
- 680 [11]. Wang F-J, Wang C-H. Sustained release of etanidazole from spray dried microspheres
681 prepared by non-halogenated solvents. *J Controlled Release*. 2002;81:263-280
- 682 [12]. Makhlof A, Tozuka Y, Takeuchi H. pH-Sensitive nanospheres for colon-specific drug delivery
683 in experimentally induced colitis rat model. *Eur J Pharm Biopharm*. 2009;72(1):1-8.
- 684 [13]. Bain DF, Munday DL, Smith A. Solvent influence on spray-dried biodegradable microspheres.
685 *J Microencapsul*. 1999;16(4):453-474.
- 686 [14]. Vehring R. Pharmaceutical particle engineering via spray drying. *Pharm Res*. 2008;25(5):999-
687 1022.
- 688 [15]. Bell SEJ, Dennis AC, Fido LA, et al. Characterization of silicone elastomer vaginal rings
689 containing HIV microbicide TMC120 by Raman spectroscopy. *J Pharm Pharmacol*.
690 2007;59(2):203-207.
- 691 [16]. Giunchedi P, Alpar HO, Conte U. PDLLA microspheres containing steroids: spray drying, o/w
692 and w/o/w emulsification as preparation methods. *J Microencapsul*. 1998;15:185-195.
- 693 [17]. Rizi K, Donaldson M, Green R, Williams A. Using pH abnormalities in diseased skin to trigger
694 and target topical therapy. *Pharm Res*: Submitted.
- 695 [18]. Sparavigna A, Setaro M, Gualandri V. Cutaneous pH in children affected by atopic dermatitis
696 and in healthy children: a multicenter study. *Skin Res Technol*. 1999;5(4):221-7.
- 697 [19]. Kendall RA, Alhnan MA, Nilkumhang S, Murdan S, Basit AW. Fabrication and in vivo
698 evaluation of highly pH-responsive acrylic microparticles for targeted gastrointestinal
699 delivery. *Eur J Pharm Sci*. 2009;37(3-4):284-290.
- 700 [20]. Healy AM, McDonald BF, Tajber L, Corrigan OI. Characterisation of excipient-free
701 nanoporous microparticles (NPMPs) of bendroflumethiazide. *Eur J Pharm Biopharm*.
702 2008;69(3):1182-1186.
- 703 [21]. Sansone F, Aquino RP, Gaudio PD, Colombo P, Russo P. Physical characteristics and aerosol
704 performance of naringin dry powders for pulmonary delivery prepared by spray-drying. *Eur J*
705 *Pharm Biopharm*. 2009;72(1):206-213.

- 706 [22]. Florey K, ed. *Triamcinolone*. New York: Academic Press; 1977. Analytical profiles of drug
707 substances; No. 1.
- 708 [23]. Ahmed A, Barry BW, Williams AC, Davis AF. Penciclovir solubility in Eudragit films: a
709 comparison of X-ray, thermal, microscopic and release rate techniques. *J Pharm Biomed*
710 *Anal.* 2004;34(5):945-956.
- 711 [24]. Rizi K, Green RJ, Donaldson M, Williams AC. Production of pH-responsive microparticles by
712 spray drying: Investigation of experimental parameter effects on morphological and release
713 properties. *J Pharm Sci.* 2010;100(2):566-579.
- 714 [25]. Friesen DT, Shanker R, Crew M, Smithey DT, Curatolo WJ, Nightingale JAS. Hydroxypropyl
715 Methylcellulose Acetate Succinate-Based Spray-Dried Dispersions: An Overview. *Mol*
716 *Pharmaceutics.* 2008;5(6):1003-1019.
- 717 [26]. Technical bulletin: Shin-Estu AQOAT: Shin-Estu Chemical Co.Ltd; 2006.
- 718 [27]. Wu P, Huang Y-B, Chang J-S, Tsai M-J, Tsai Y-H. Design and evaluation of sustained release
719 microspheres of potassium chloride prepared by Eudragit®. *Eur J Pharm Sci.* 2003;19:115-
720 122.
- 721 [28]. Pignatello R, Bucolo C, Ferrara P, Maltese A, Puleo A, Puglisi G. Eudragit RS100
722 nanosuspensions for the ophtalmic controlled delivery of ibuprofen. *Eur J Pharm Sci.*
723 2002;16:53-61.
- 724 [29]. Meissner Y, Pellequer Y, Lamprecht A. Nanoparticles in inflammatory bowel disease:
725 particles targeting versus pH-sensitive delivery. *Int J Pharm.* 2006;316:138-143.
- 726 [30]. Lamprecht A, Yamamoto H, Takeuchi H, Kawashima Y. Design of pH-sensitive microspheres
727 for the colonic delivery of the immunosuppressive drug tacrolimus. *Eur J Pharm Biopharm.*
728 2004;58(1):37-43.
- 729 [31]. Lamprecht A, Yamamoto H, Takeuchi H, Kawashima Y. pH-sensitive microsphere delivery
730 increases oral bioavailability of calcitonin. *J Controlled Release.* 2004;98:1-9.
- 731 [32]. Rowe RC, Sheskey PJ, Owen SC, (ed). *Handbook of pharmaceutical excipients*. 5th ed:
732 Pharmaceutical Press; 2006.
- 733 [33]. Yang M, Cui F, You B, et al. A novel pH-dependent gradient-release delivery system for
734 nitrendipine: I. Manufacturing, evaluation in vitro and bioavailability in healthy dogs. *J*
735 *Controlled Release.* 2004;98(2):219-229.
- 736 [34]. You J, Cui F-d, Li Q-p, Han X, Yu Y-w, Yang M-s. A novel formulation design about water-
737 insoluble oily drug: preparation of zedoary turmeric oil microspheres with self-emulsifying
738 ability and evaluation in rabbits. *Int J Pharm.* 2005;288(2):315-323.
- 739 [35]. Sato Y, Kawashima Y, Takeuchi H, Yamamoto H. Physicochemical properties to determine
740 the buoyancy of hollow microparticles (microballons) prepared by the emulsion solvent
741 diffusion method. *Eur J Pharm Biopharm.* 2003;55:297-304.
- 742 [36]. Augsburger LL, Hoag SW. *Pharmaceutical Dosage Forms: Unit operations and mechanical*
743 *properties*. Vol 1. 3rd ed: Informa Health Care; 2008.
- 744 [37]. Siepmann J, Faisant N, Akiki J, Richard J, Benoit P. Effect of the size of biodegradable
745 microparticles on drug release: experiment and theory. *J Controlled Release.* 2004; 96(1):
746 123-134.
- 747 [38]. Kim EH-J, Chen XD, Pearce D. On the mechanisms of surface formation and the surface
748 compositions of industrial milk powders. *Drying Technol.* 2003;21(2):265 - 278.
- 749 [39]. Nilkumhang S, Alhnan MA, McConnell EL, Basit AW. Drug distribution in enteric
750 microparticles. *Int J Pharm.* 2009;379(1):1-8.
- 751 [40]. Vanber R. Formation and physical characterisation of large porous particles for inhalation.
752 *Pharm Res.* 1999;16(11):1735-1742.
- 753 [41]. Nilkumhang S, Basit AW. The robustness and flexibility of an emulsion solvent evaporation
754 method to prepare pH-responsive microparticles. *Int J Pharm.* 2009;377(1-2):135-141.
- 755 [42]. Yadav A, Yadav V. Preparation and evaluation of polymeric carbamazepine spherical crystals
756 by emulsion solvent diffusion technique. *Asia J Pharm.* 2009; 3: 18-25.

- 757 [43]. Dubernet C. Thermoanalysis of microspheres. *Thermochim Acta*. 1995;248:259.
- 758 [44]. Lin S-Y, Liao C-M, Husiue G-H, Liang R-C. Study of a theophylline-Eudragit L mixture using a
759 combined system of microscopic Fourier-transform infrared spectroscopy and differential
760 scanning calorimetry. *Thermochimica Acta*. 1995;245(153-166).
- 761 [45]. Velaga SP, Ghaderi R, Carlfors J. Preparation and characterisation of hydrocortisone particles
762 using a supercritical fluids extraction process. *Int J Pharm*. 2002;231(2):155-166.
- 763 [46]. Fleming OS, Chan KLA, Kazarian SG. FT-IR imaging and Raman microscopic study of
764 poly(ethylene terephthalate) film processed with supercritical CO₂. *Vil Spectrosc*. 2004;35(1-
765 2):3-7.
- 766 [47]. Salmain M, Vessières A, Top S, Jaouen G, Butler IS. Analytical potential of near-infrared
767 fourier transform Raman spectra in the detection of solid transition metal carbonyl steroid
768 hormones. *J Raman Spectrosc*. 1995;26(1):31-38.
- 769 [48]. Socrates G. *Infrared and Raman characteristic group frequencies: tables and charts*. 3rd ed.
770 Chichester: John Wiley & Sons; 2001.
- 771 [49]. Pelletier MJ, ed. *Analytical applications of Raman spectroscopy*. 1st ed. Oxford: Blackwell
772 Science; 1999.